Author Manuscript

Author Manuscript

Author Manuscript

Author Manuscript

HHS Public Access

Author manuscript

J Phys Chem C Nanomater Interfaces. Author manuscript; available in PMC 2018 December 28.

Published in final edited form as:

J Phys Chem C Nanomater Interfaces. 2017 December 28; 121(51): 28425–28434. doi:10.1021/acs.jpcc.7b11485.

Spin Relays Enable Efficient Long-Range Heteronuclear Signal Amplification By Reversible Exchange

Roman V. Shchepin[a], **Lamya Jaigirdar**[a,b], **Thomas Theis**[c], **Warren S. Warren**[c], **Boyd M. Goodson**[d], and **Eduard Y. Chekmenev**[a,e,f,*]

[a]Vanderbilt University Institute of Imaging Science (VUIIS), Department of Radiology, Vanderbilt University Medical Center (VUMC), Nashville, Tennessee 37232-2310 United States

[b]Vanderbilt University, School of Engineering, Nashville, Tennessee 37232 United States

[c]Department of Chemistry, Duke University, Durham, North Carolina 27708, United States

[d]Department of Chemistry and Biochemistry and Materials Technology Center, Southern Illinois University, Carbondale, Illinois 62901, United States

[e]Department of Biomedical Engineering, Vanderbilt University, Vanderbilt-Ingram Cancer Center (VICC), Nashville, Tennessee 37232-2310, United States

[f]Russian Academy of Sciences, Leninskiy Prospekt 14, Moscow, 119991, Russia

Abstract

A systematic experimental study is reported on the polarization transfer to distant spins, which do not directly bind to the polarization transfer complexes employed in Signal Amplification By Reversible Exchange (SABRE) experiments. Both, long-range transfer to protons and long-range transfer to heteronuclei i.e. ^{13}C and ^{15}N are examined. Selective destruction of hyperpolarization on ^{1}H, ^{13}C, and ^{15}N sites is employed, followed by their re-hyperpolarization from neighboring spins within the molecules of interest (pyridine for ^{1}H studies and metronidazole-$^{15}N_2$-$^{13}C_2$ for ^{13}C and ^{15}N studies). We conclude that long-range sites can be efficiently hyperpolarized when a network of spin-½ nuclei enables relayed polarization transfer (*i.e.* via short-range interactions between sites). In case of proton SABRE in the milli-Tesla regime, a relay network consisting of protons only is sufficient. However, in case ^{13}C and ^{15}N are targeted (i.e. via SABRE in SHield Enables Alignment Transfer to Heteronuclei or SABRE-SHEATH experiment), the presence of a heteronuclear network (*e.g.* consisting of ^{15}N) enables a relay mechanism that is significantly more efficient than the direct transfer of spin order from *para*-H_2-derived hydrides.

Graphical Abstract

*Corresponding Author: eduard.chekmenev@vanderbilt.edu.

Supporting Information

The Supporting Information is available free of charge on the ACS Publications website.

Additional supporting Figures (PDF).

Detailed Tables summarizing computation of signal enhancements (PDF).

Author Manuscript Author Manuscript Author Manuscript Author Manuscript

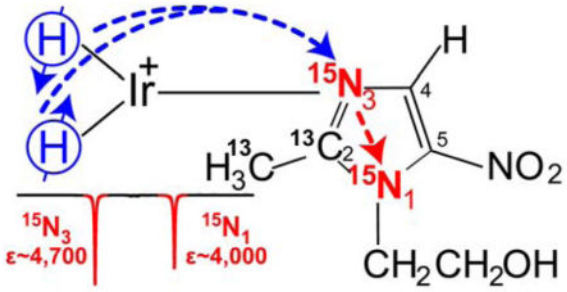

INTRODUCTION

Hyperpolarization techniques transiently increase nuclear spin polarization (*P*) by several orders of magnitude, resulting in corresponding gains in NMR signals.[1] These techniques[2] enable new applications including *in vivo* molecular imaging,[3–6] which relies on preparation, administration, and MRI of exogenous hyperpolarized (HP) contrast agents. Several technologies have been developed to produce HP states of low-gamma spin 1/2 nuclei (*e.g.* ^{13}C and ^{15}N), which retain HP state significantly longer than protons in biomolecular motifs.

Signal Amplification by Reversible Exchange (SABRE)[7] is the hyperpolarization method, which employs parahydrogen (*para*-H_2) as the source of spin order.[8] SABRE relies on spontaneous polarization transfer from *para*-H_2-derived hydrides to a substrate on polarization transfer catalysts. The SABRE polarization transfer is primarily accomplished via spin-spin interactions (*i.e.* J-couplings). While other interactions may contribute, they are generally orders of magnitude less efficient.[9–11] When polarization transfer is performed in milli-Tesla (mT) magnetic fields, the polarization from *para*-H_2-derived hydrides is spontaneously transferred to proton sites in substrates, enabling ^1H polarization values (%P_H) of up to 50%.[12] In this case, proton-proton spin-spin couplings ($J_{H\text{-}H}$) enable SABRE polarization transfer.[7, 11, 13] Another variant of this technique dubbed SABRE in SHield Enables Alignment Transfer to Heteronuclei (SABRE-SHEATH) is an efficient process for hyperpolarizing ^{15}N sites, in one example providing more than 20% polarization in 1 minute.[14] ^{15}N-hyperpolarization is of particular interest, because it enables long hyperpolarization lifetimes and exponential decay constants. In some cases, ^{15}N exponential decay constant can exceed 20 minutes.[15–16] SABRE-SHEATH is accomplished at micro-Tesla (μT) magnetic fields, enabling spontaneous polarization transfer from *para*-H_2-derived hydrides to heteronuclei, as illustrated in Scheme 1a. In case of ^{15}N SABRE-SHEATH protonnitrogen-15 spin-spin couplings ($J_{H\text{-}15N}$) enable the spontaneous polarization transfer.[17–18] While polarization transfer between nuclear spins in the same molecule in solution is an extremely well documented area, the case is less clear for SABRE and SABRE-SHEATH, which occur within a complex with finite lifetime, and which involves several changes of the external magnetic field.

Over the past two years, this approach has been bolstered by a series of advancements from proof-of-principle demonstrations in organic solvents[17–18] (including “neat” substrates[19]) all the way to demonstrations of SABRE-SHEATH enhancement under heterogeneous catalytic

Author Manuscript Author Manuscript Author Manuscript Author Manuscript

conditions[20] and catalysis in aqueous media,[21] which in principle will enable the preparation of pure aqueous ^{15}N HP compounds for potential *in vivo* use. Moreover, the scope of amendable bio-structures has been expanded from N-heterocycles to Schiff bases,[22] diazirines,[15] and nitriles.[16]

However, despite these successes, to date SABRE-SHEATH has been primarily employed for hyperpolarization of ^{15}N sites that bind directly to metal centers via two-bond spin-spin couplings (*i.e.* short-range couplings to substrate ^{15}N sites directly binding to catalysts like Ir-IMes [IMes = 1,3-bis(2,4,6-trimethylphenyl)imidazole-2-ylidene], Scheme 1a).[23] Efforts to hyperpolarize long-range ^{15}N sites (*i.e.* more than 2 chemical bonds away from *para*-H_2-hydrides) showed that polarization efficiency is reduced by more than an order of magnitude[14]—presenting a clear obstacle for expanding SABRE hyperpolarization technology to broader classes of substrates. Moreover, recent studies of direct ^{13}C[24 and 19]F[25] hyperpolarization via SABRE indicated that the problem can be mitigated if the nitrogen sites binding the iridium metal centers are labeled with ^{15}N nuclei as opposed to naturally occurring quadrupolar ^{14}N spins.[24] However, the obvious question regarding the mechanism of polarization transfer (and more importantly its limitations) was unanswered. Specifically: “Is SABRE of distant heteronuclei accomplished directly via long-range *J*-couplings, or does it work indirectly via relay through a network of spins (Scheme 1b)? Here, we present experimental evidence that SABRE of long-range ^{15}N and ^{13}C sites is efficient in the presence of a relay network connected by close-range spin-spin couplings. While the data presented does not rule out a direct mechanism via weak long-range *J*-couplings, the indirect mechanism is significantly more efficient than the direct polarization transfer (i.e., the enhancements observed cannot be fully explained by long-range transfer; although long-range transfer is possible, it leads to weaker enhancements). We hope that the presented work will stimulate future theoretical studies and pave the way to efficient SABRE-SHEATH hyperpolarization of remote heteronuclear sites thereby expanding the reach of this technique.

METHODS

All NMR spectra were recorded using a 9.4 T Bruker Avance III high-resolution NMR spectrometer equipped with a broad-band dual-channel NMR probe. All SABRE experiments were performed using ~50% *para*-H_2. All sample manipulations related to the sample transfer between magnetic fields (*i.e.* the Magnetic Field Cycling (MFC) procedures) were performed manually (Figures 1a,b and 2a,b). The NMR spectra from metronidazole-$^{15}N_2$-$^{13}C_2$ (Millipore-Sigma P/N 32744-10MG) samples were recorded in medium-wall 5 mm NMR tubes, whereas the spectra from signal reference samples were recorded using standard 5 mm NMR tubes.

Preparation of solutions

Previously synthesized IrIMes catalyst was used for the described studies.[10] Metronidazole-$^{15}N_2$-$^{13}C_2$ (~20 mM final concentration) and pre-activated iridium catalyst ([IrCl(COD)(IMes)], ~1.0 mM final concentration) and methanol-d_4 were prepared from stock solutions of Metronidazole-$^{15}N_2$-$^{13}C_2$ (40 mM) and ([IrCl(COD)(IMes)], 2.0 mM).

Author Manuscript Author Manuscript Author Manuscript Author Manuscript

Both solutions were flushed with Argon and vortexed (at least three times) in an Eppendorf safe-lock tube and Duran bottle (10 mL GL25) correspondently. Please note: while Metronidazole-$^{15}N_2$-$^{13}C_2$ solution was used over a period of several days (stored at ~6 C°), ([IrCl(COD)(IMes)] was prepared fresh each day and stored for <10 hours in a refrigerator (~6 C°). A portion (~0.3 mL) of each stock solutions was transferred into an Argon-filled medium-walled 5 mm NMR sample tube: 9 in.-long, 3.43-mm inner diameter (ID) (Wilmad Glass, P/N 503-PS-9) equipped with a Teflon tube extension: 0.25 in. outer diameter (OD), 3/16 in. ID. The Teflon extension was approximately 3-in. long. The tube was connected to the previously described setup.[27] The best results were obtained by SABRE sample activation by bubbling *para*-H_2 for ~3 minutes (at 90 sccm & 65 psi) and leaving sample for ~1 hour under *para*-H_2 at 65 psi.

SABRE hyperpolarization

For SABRE experiments, the *para*-H_2 flow rate (50 sccm, ~1 minute of bubbling) was controlled using a mass flow controller (Sierra Instruments, Monterey, CA, P/N C100L-DD-OV1-SV1-PV2-V1-S0-C0). The schematic of SABRE experimental setup is shown in Figure 1a, and the corresponding sequence of the events is shown in Figure 1b. Micro-Tesla magnetic field was created by attenuating the Earth's magnetic field using a three-layered mu-metal shield (Magnetic Shield Corp., Bensenville, IL, P/N ZG-206,). The tuning of SABRE-SHEATH magnetic field was achieved by custom-built solenoid coil (>90% homogeneity over >15 cm length) and a power supply (GW INSTEK, GPRS series) with variable-resistor bank connected in series with the magnet coil. When *para*-H_2 bubbling was stopped, the sample was transferred from the shield to the Earth's magnetic field (*ca*. 50 μT), followed by rapid sample transfer into a 9.4 T magnet of the NMR spectrometer for data acquisition or further manipulations as described in the main text. Typical sample transfer time (from cessation of *para*-H_2 gas to $^{15}N/^{13}C/^{1}H$ signal detection) was 4–7 seconds. The schematic of SABRE-SHEATH experimental setup is shown in Figure 2a, and the corresponding sequence of the events is shown in Figure 2b.

The reader should note use of magnetic field cycling (MFC) to the Earth's magnetic field, *ca*. 50 μT, (SABRE-SHEATH, Figure 2b) for ^{15}N re-polarization, whereas ^{1}H re-polarization (SABRE, Figure 1b) employs MFC to the fringe field, *ca*. 6 mT, due to the difference in the matching conditions for efficient $^{15}N \rightarrow {}^{15}N$ or $^{1}H \rightarrow {}^{1}H$ re-polarization respectively: see the main text for more detailed consideration.

Computation of NMR signal and nuclear spin polarization enhancements

The signal enhancements were computed as the following. ^{1}H enhancements were computed by diving the HP signal magnitude by the magnitude of thermally polarized signals. In case of ^{15}N and ^{13}C, the thermally polarized signals were generally very low, and therefore, external signal reference was employed. The enhancements were computed as follows:

$$\varepsilon = \frac{S_{HP}}{S_{REF}} \times \frac{C_{REF}}{C_{HP}} \times \frac{A_{REF}}{A_{HP}} \times \frac{N_{REF}}{N_{HP}}$$

Author Manuscript Author Manuscript Author Manuscript Author Manuscript

where S_{HP} and S_{REF} are NMR signals for HP state and thermally polarized signal reference samples respectively, C_{REF} and C_{HP} are the effective isotope concentrations of thermally polarized signal reference and HP samples respectively, A_{REF} and A_{HP} are the solution cross-sections in the NMR tube of thermally polarized signal reference and HP samples respectively, and N_{REF} and H_{HP} are the numbers of symmetrical sites per molecule for the thermally polarized signal reference and HP samples respectively (A_{REF}/A_{HP} was ~1.85 as described earlier[18]). Percentage polarization was computed by multiplying signal enhancement ε by the equilibrium nuclear spin polarization of a given spin at 9.4T and 298K: 3.2×10^{-3}% (^{1}H), 8.1×10^{-4}% (^{13}C), 3.3×10^{-4}% (^{15}N).

RESULTS AND DISCUSSION

General Consideration

Briefly, the reader is reminded that in case of traditional SABRE (i.e. hyperpolarization of proton sites), the matching condition for *J*-coupling (^{1}H-^{1}H) mediated polarization transfer occurs at a few mT magnetic field. In case of SABRE-SHEATH (i.e. hyperpolarization of heteronuclear sites, e.g. ^{15}N and ^{13}C), the matching condition for *J*-coupling (e.g., ^{1}H-^{15}N) mediated polarization transfer occurs at μT magnetic field. Detailed theory is provided in earlier works of Duckett et al.[7, 11, 13] and Theis at al.[17–18]

SABRE hyperpolarization of pyridine proton sites

The first reports of SABRE demonstrated that proton sites at least six-bonds away can be efficiently hyperpolarized.[7, 13] The theoretical basis for SABRE[11] indicated that polarization transfer from *para*-H_2-hydrides to substrate protons is accomplished via a networks of proton-proton couplings, although the recent study by Eshuis and co-workers determined the values of these four-, five-, and six-bond spin-spin couplings, and postulated that these long-range couplings may also enable the canonical SABRE effect via the direct transfer of spin order.[28]

Here, we have employed the approach previously described for studying ^{1}H SABRE,[27] and performed selective spin destruction of HP resonances of *ortho*-pyridine protons (denoted as Ha in Figure 3a) after the sample was hyperpolarized at magnetic field of ~6 mT and *para*-H_2 bubbling was stopped (Figure 3b). After destroying the Ha polarization with a frequency-selective pulse (Figure 3c), the sample was moved back into the ~6 mT field, and finally, the sample was returned to the 9.4 T NMR spectrometer for detection (this procedure effectively represents magnetic field cycling or MFC – the details of the experimental setup and the involved steps are shown in Figure 1a,b of the Methods section). The resulting spectrum shown in Figure 3d indeed shows that the Ha HP state is successfully recreated using the *meta*- and *para*- (Hb and Hc) protons as hyperpolarization reservoirs. Corresponding datasets showing HP state destruction and re-creation for the Hb and Hc protons may be found in the Supporting Information (Figure S1).

All-in-all, the experimental results shown in Figure 3a,b,c,d and Figure S1 are clearly consistent with the canonical (*i.e.* ^{1}H) SABRE effect in the mT regime may indeed rely on

Author Manuscript Author Manuscript Author Manuscript Author Manuscript

the network of proton-proton couplings, in agreement with pioneering studies by Duckett and co-workers.[7, 11, 13]

SABRE hyperpolarization of metronidazole-$^{15}N_2$-$^{13}C_2$ in micro-Tesla (μT) magnetic fields (SABRE-SHEATH)

Hyperpolarization in μT magnetic fields was performed using a μ-metal magnetic shield that attenuates the Earth's magnetic field (*ca.* 50 μT) down to the sub-μT regime (Figure 2a).[17–18, 29] The structure of the activated complex and the schematic of SABRE-SHEATH process are shown in Scheme 2. Efficient ^{15}N[17–18 and] ^{13}C[24] SABRE-SHEATH hyperpolarization has been demonstrated previously, and no significant effort was made to optimize polarization parameters (*e.g.*, temperature and μT field) for the present study.

The following polarization levels were achieved for ~20 mM metronidazole-$^{15}N_2$-$^{13}C_2$ solutions in methanol-d_4 using 50% *para*-H_2:[30] ε_{15N1} ~ 4,000 (%P_{15N1}~1.3%), ε_{15N3} ~ 4,700 (%P_{15N1}~1.5%), Figure 4a,b, ε_{13C2} ~ 310 (%P_{13C2}~0.3%), ε_{13CH3} ~ 230 (%P_{13CH3}~0.2%), Figure 4c,d, ε_H ~ 14 (%P_H~0.o4%), Figure 4e,f,g. If near 100% *para*-H_2 were employed, the polarization values would be effectively tripled. %P_{15N} values are within the expected ranges for the employed concentration regime.[17–18] %P_{13C} values are several times lower than %P_{15N}, because initial micro-Tesla field optimization was performed for ^{15}N spins, and the optimization of polarization efficiency was outside the scope of the presented mechanistic study. %P_H values are significantly lower than %P_{15N} and %P_{13C} values, because μT fields are not optimal for proton SABRE.

SABRE-SHEATH hyperpolarization of long-range ^{15}N sites

^{15}N hyperpolarization of metronidazole[14] at natural abundance of ^{15}N (~0.3%) and ^{13}C (~1.1%) isotopes was recently shown. In that work, the efficiency of SABRE-SHEATH hyperpolarization (gauged as %P_{15N}) of $^{15}N_1$ and -$^{15}NO_2$ sites was significantly lower (by more than an order of magnitude) than that of the $^{15}N_3$ site. Low natural $^{13}C/^{15}N$ abundance results in simplification of the spin system (participating in SABRE-SHEATH), effectively reducing it to a three-spin system (Scheme 3), because the statistical probability of the simultaneous presence of two spins (*e.g.* ^{15}N and ^{15}N or ^{15}N and ^{13}C) is two orders of magnitude lower than the statistical probability of the structures shown in Scheme 3a–c (Note, SABRE relevant spin-spin couplings for direct polarization transfer are shown in Scheme 3e,f).

The ^{15}N SABRE-SHEATH polarization of met-ronidazole-$^{15}N_2$-$^{13}C_2$ shows that polarization efficiency of $^{15}N_1$ site is 85% of that of the $^{15}N_3$ site (Figure 4a), which is markedly different from the previously reported corresponding value of 2%.[14] This more than 40-fold improvement of hyperpolarization at $^{15}N_1$ can be rationalized by the presence of $^{15}N_3$ and ^{13}C sites in this labeled molecule, which provide a J-coupling network enabling relayed SABRE-SHEATH polarization transfer (instead of direct H→$^{15}N_1$ transfer). In the relayed case, two-bond couplings ($^2J_{H\text{-}15N3}$ and $^2J'_{H\text{-}15N3}$) enable hyperpolarization of the $^{15}N_3$ site, and ^{15}N hyperpolarization is then propagated to other ^{13}C and ^{15}N sites via the heteronuclear coupling network.

Author Manuscript Author Manuscript Author Manuscript Author Manuscript

Additional experimental evidence for the relayed nature of such polarization transfer is provided in Figures 5 and 6. For these experiments the HP sample was inserted in the 9.4 T NMR spectrometer and the $^{15}N_3$ hyperpolarization was destroyed using frequency-selective RF pulses (note that the $^{15}N_1$ polarization was preserved in this case, Figure 5a). The relevant setup and sample manipulation steps are shown in Figure 2b. Following this selective polarization-destruction procedure, the sample was transferred into the Earth's magnetic field (*ca.* 50 μT) to enable 're-mixing' of heteronuclear polarization (*no* bubbling of fresh *para*-H_2 is performed). Lastly, the sample was returned into the NMR spectrometer for read-out. After this magnetic field cycling (MFC), the polarization of $^{15}N_3$ is recovered to nearly the same level as the one for the $^{15}N_1$ site, as shown in Figure 5b. We note that the T_1 of ^{15}N sites is typically on the order of 1 minute or greater, and a significant fraction of hyperpolarization can be retained after 10–30 seconds of manipulation time required in such experiments. We also note that *para*-H_2 bubbling employed in the initial SABRE-SHEATH procedure was stopped before the sample left the magnetic shield for the first time. We also note that even when the SABRE hyperpolarization experiment was performed at the (higher) Earth's magnetic field (control experiment), the achieved polarization on $^{15}N_1$ and $^{15}N_3$ sites (Figure 5c) was lower than the one achieved in Figure 5b. When combined, this evidence supports the conclusion that in the MFC procedure, the $^{15}N_3$ site was re-hyperpolarized using the hyperpolarization pool of the $^{15}N_1$ site. While some polarization transfer from ^{13}C is also potentially possible, it is less likely because HP ^{13}C sites depolarize more quickly and the initial polarization levels of ^{13}C sites were significantly lower than those of ^{15}N sites (Figure 4a). Moreover, in a separate experiment, we inverted (using a 180° RF pulse) ^{15}N magnetization of the HP $^{15}N_1$ site (Figure 5d) prior to the second MFC procedure. As a result of the spin inversion of the $^{15}N_1$ site, the resulting polarization on the $^{15}N_3$ site followed this inversion (Figure 5e) after MFC. Furthermore, additional experiments (Figure S2b) shows that MFC to the fringe field of ~6 mT was not sufficient to achieve this effect, and re-hyperpolarization was less efficient.

The re-hyperpolarization mechanism requires mixing of spin states from $^{15}N_3$ and $^{15}N_1$ sites. At the Earth's field (*ca.* 50 μT) the chemical shift difference of the two sites (ca. 100 ppm away) is only ~0.02 Hz, which is significantly less than their *J*-coupling (which we estimate to be on the order of a Hertz or less). At 6 mT the frequency difference of the two sites is ~2.6 Hz, which is apparently still too large for efficient level anti-crossing. Accordingly, MFC to the Earth's field (*ca.* 50 μT) is required.[31–33] We also note that performing the MFC procedure from the 9.4 T to the magnetic shield (and therefore passing the Earth's field condition twice) also leads to the ^{15}N re-polarization (data not shown), but the effect is significantly reduced, which is likely due to additional polarization leaks (e.g. to ^{13}C and ^{1}H sites).

Figure 6 provides additional experimental evidence for polarization transfer from $^{15}N_3$ site to $^{15}N_1$ site. Instead of applying the frequency-selective irradiation on $^{15}N_3$, it was applied to $^{15}N_1$ (Figure 6a). Exactly analogous results are obtained. The MFC to Earth's field (*ca.* 50 μT) enables re-hyperpolarization of $^{15}N_1$ using the polarization of HP $^{15}N_3$ (Figure 6b). The corresponding spin inversion experiments (Figure 6c,d) prove that $^{15}N_1$ site was indeed re-hyperpolarized from magnetization of HP $^{15}N_3$ site.

Author Manuscript Author Manuscript Author Manuscript Author Manuscript

While the possibility of polarization transfer between spin ½ nuclei is predictable, *e.g.* between two ^{15}N spins as shown here), demonstrating this phenomenon in the context of SABRE/SABRE-SHEATH repolarization is critical for understanding and proving the mechanism of relayed polarization transfer in weak magnetic fields. Taken together, the above evidence supports the model of relayed ^{15}N SABRE-SHEATH polarization of long range sites, explaining the efficient polarization of a distant $^{15}N_1$ site that is four bonds away from the *para*-H_2-derived metal hydrides (Scheme 3d).

SABRE-SHEATH hyperpolarization of long-range ^{13}C sites

Figure 4c demonstrates the efficient SABRE-SHEATH hyperpolarization of ^{13}C sites three and four bonds away from *para*-H_2-derived hydrides. Importantly, the efficiency of ^{13}C hyperpolarization of the-$^{13}\underline{C}H_3$ group was ~75% of that of $^{13}C_2$ site; we note however, that –$^{13}\underline{C}H_3$ sites may have lost disproportionately more polarization during sample transfer from μT field to 9.4 T of NMR spectrometer, because the ^{13}C T_1 in methyl groups is typically significantly shorter than T_1 values of ^{13}C sites without directly attached protons (*e.g.* the $^{13}C_2$ site). Therefore, the actual efficiency (at the end of the SABRE-SHEATH procedure prior to the HP sample transfer) might have been better than 75%. We have recently demonstrated that the presence of a ^{15}N nucleus in pyridine and other similar compounds is essential for efficient polarization (*i.e.* large $\%P_{13C}$ values) of ^{13}C sites that are three (*ortho*-position) and four (*meta*-position, Figure 3) chemical bonds away from hydride protons (Scheme 1).[24] That previous proof-of-principle work did not address the reasons for low heteronuclear polarization efficiency in the case of ^{14}N spins that would otherwise be present in such compounds. One part of the explanation is enhanced scalar relaxation of the second kind[34–37] suffered by the target spins within the micro-Tesla regime, induced by quadrupolar ^{14}N sites within the scalar coupling network. A second explanation is the absence of a close spin ½ *J*-coupling network. All-in-all, the data presented in Figure 7 supports the importance of *J*-coupling networks for hyperpolarization of ^{13}C spins too (in addition to the ^{15}N sites discussed as the primary topic of this work).

In Figure 7 we provide additional evidence supporting the need for polarization relays in such strongly coupled networks. First, a metronidazole-$^{15}N_2$-$^{13}C_2$ sample was hyperpolarized via SABRE-SHEATH and *para*-H_2 bubbling was stopped. Next, the sample was rapidly transferred into the 9.4 T NMR spectrometer, and hyperpolarization on the ^{13}C and ^{1}H sites was immediately destroyed (by applying a series of 90° RF pulses to ^{13}C spins and ^{1}H decoupling to ^{1}H spins) and a proton-decoupled ^{13}C spectrum was acquired (Figure 7a). In a separate experiment (instead of recording ^{13}C spectrum), the sample was additionally transferred back into the μT field created by the magnetic shield (employed for SABRE-SHEATH polarization in the first step—here employed to re-enable heteronuclear polarization transfer), and ^{13}C hyperpolarization was indeed re-created (Figure 7b). Note that since all ^{13}C and ^{1}H sites were depolarized (by broadband irradiation), we conclude that the only remaining source of polarization for such ^{13}C re-hyperpolarization is the hyperpolarization pool of ^{15}N sites. Moreover, the efforts to re-polarize this sample by MFC to the Earth's magnetic field (Figure 7c) were unsuccessful in comparison to re-hyperpolarization at μT field (Figure 7b)—further indicating that the source of polarization must be from non-carbon spins.

Author Manuscript Author Manuscript Author Manuscript Author Manuscript

Broader relevance

Metronidazole is an important potential contrast agent (because high $\%P_{15N}$ can be achieved,[14] and it is possible to administer high (~2 g[38]) dose of this potent antibiotic) that can be potentially employed for hypoxia imaging in a manner similar to fluoromisonidazole (FMISO) and other radiolabeled nitroimidazole derivatives[39–44] used in position emission tomography (PET) imaging. Therefore, this work will certainly be useful for future development and optimization of SABRE-SHEATH hyperpolarization of this and other ^{15}N and ^{13}C HP imaging probes.

More generally, the systematic studies presented in this work provide clear experimental evidence that heteronuclear *J*-coupling spin-1/2 networks serve as the underlying fundamental basis for efficient *relayed* polarization transfer from *para*-H_2-derived metal hydrides (Scheme 2) to substrate heteronuclei that do not directly bind to the Iridium complex. Here, we show that efficient hyperpolarization of long-range ^{13}C and ^{15}N sites is achieved in SABRE when a network of heteronuclear *J*-couplings is present. The presence of this network translates to efficient hyperpolarization of many heteronuclei, including ^{13}C, ^{24} ^{15}N,[17] ^{31}P,[45,] ^{19}F,[25] etc.[46]. Most importantly, the nitrogen site directly interacting with the iridium hexacoordinate complex should be labeled to create a relay of spin ½ nuclei for efficient polarization transmission deeper within the intramolecular space. Therefore, we believe this relayed mechanism opens new opportunities for efficient SABRE hyperpolarization of new biomolecular targets, and informs the rational design of nuclear spin coupling networks in labeled agents for a wide variety of potential biomedical applications. Of note, ^{13}C labeling did not significantly affect ^{15}N T_1 relaxation: $T_1(^{15}N_3)$ is *ca.* 36 s with (data not shown) and without ^{13}C spin labeling[14], which is relevant for production of HP contrast agents with long-lived HP states in the context of biomedical applications. As another example, uniformly (or backbone-) $^{13}C/^{15}N$ labeled peptides and proteins can potentially act as efficient networks of SABRE hyperpolarization, and it may be possible to hyperpolarize isotopically labeled peptides and proteins using this approach. We also envision that isotopically labeled DNA, RNA, and other structures can be hyperpolarized via this SABRE-SHEATH approach. The general concept of relayed polarization transfer through a close *J*-coupling network will also potentially translate to LIGHT-SABRE and RF-SABRE sequences that create hyperpolarization directly in the magnet and avoid the need for sample transfer.[47–49]

In the context of SABRE hyperpolarization of *proton* sites, this work provides experimental evidence in support of relayed polarization transfer. As a result, it would be potentially possible to hyperpolarize long-range proton sites too. While proton-hyperpolarized compounds are rarely used for contrast agents for HP MRI, potential SABRE applications most likely would include analysis of complex mixtures at low concentrations[50–53] with potential detection of nitrogen- and sulfur-containing heterocycles[54] in oil or refined petroleum products.

CONCLUSION

Efficient SABRE hyperpolarization of long-range ^{13}C and ^{15}N sites was demonstrated in metronidazole-$^{15}N_2$-$^{13}C_2$ in the μT field regime. We have shown that long range ^{13}C and

Author Manuscript Author Manuscript Author Manuscript Author Manuscript

^{15}N sites (*i.e.* three and four chemical bonds away from *para*-H_2-derived hydrides) can be hyperpolarized much more efficiently via a mechanism of relayed spin-polarization transfer than via weak long-range *J*-couplings. Specifically, the short-range ^{15}N site, directly bound to Iridium, is hyperpolarized first and hyperpolarization is then transferred / relayed to other intramolecular sites via a network of short-range *J*-couplings involving further spins. The presented evidence opens new opportunities for SABRE-based hyperpolarization of long range spin-½ nuclei in a wide range of applications ranging from biomedical contrast agents, to analysis of complex mixtures, to structural biology.

Supplementary Material

Refer to Web version on PubMed Central for supplementary material.

Acknowledgments

This work was supported by NSF under grants CHE-1058727, CHE-1363008, CHE-1416268, and CHE-1416432, NIH 1R21EB018014, 1R21EB020323, and 1R21CA220137, DOD CDMRP BRP W81XWH-12-1-0159/BC112431, DOD PRMRP awards W81XWH-15-1-0271 and W81XWH-15-1-0272, and Exxon Mobil Knowledge Build. B.M.G. acknowledges additional support from SIUC MTC and OSPA.

References

1. Nikolaou P, Goodson BM, Chekmenev EY. NMR Hyperpolarization Techniques for Biomedicine. Chem Eur J. 2015; 21:3156–3166. [PubMed: 25470566]
2. Kurhanewicz J, Vigneron DB, Brindle K, Chekmenev EY, Comment A, Cunningham CH, DeBerardinis RJ, Green GG, Leach MO, Rajan SS, et al. Analysis of Cancer Metabolism by Imaging Hyperpolarized Nuclei: Prospects for Translation to Clinical Research. Neoplasia. 2011; 13:81–97. [PubMed: 21403835]
3. Nelson SJ, Kurhanewicz J, Vigneron DB, Larson PEZ, Harzstark AL, Ferrone M, van Criekinge M, Chang JW, Bok R, Park I, et al. Metabolic Imaging of Patients with Prostate Cancer Using Hyperpolarized 1-C-13 Pyruvate. Sci Transl Med. 2013; 5:198ra108.
4. Day SE, Kettunen MI, Gallagher FA, Hu DE, Lerche M, Wolber J, Golman K, Ardenkjaer-Larsen JH, Brindle KM. Detecting Tumor Response to Treatment Using Hyperpolarized C-13 Magnetic Resonance Imaging and Spectroscopy. Nat Med. 2007; 13:1382–1387. [PubMed: 17965722]
5. Golman K, Axelsson O, Johannesson H, Mansson S, Olofsson C, Petersson JS. Parahydrogen-Induced Polarization in Imaging: Subsecond C-13 Angiography. Magn Reson Med. 2001; 46:1–5. [PubMed: 11443703]
6. Golman K, in't Zandt R, Thaning M. Real-Time Metabolic Imaging. Proc Natl Acad Sci U S A. 2006; 103:11270–11275. [PubMed: 16837573]
7. Adams RW, Aguilar JA, Atkinson KD, Cowley MJ, Elliott PIP, Duckett SB, Green GGR, Khazal IG, Lopez-Serrano J, Williamson DC. Reversible Interactions with Para-Hydrogen Enhance NMR Sensitivity by Polarization Transfer. Science. 2009; 323:1708–1711. [PubMed: 19325111]
8. Bowers CR, Weitekamp DP. Transformation of Symmetrization Order to Nuclear-Spin Magnetization by Chemical-Reaction and Nuclear-Magnetic-Resonance. Phys Rev Lett. 1986; 57:2645–2648. [PubMed: 10033824]
9. Kovtunov KV, Kidd BE, Salnikov OG, Bales LB, Gemeinhardt ME, Gesiorski J, Shchepin RV, Chekmenev EY, Goodson BM, Koptyug IV. Imaging of Biomolecular NMR Signals Amplified by Reversible Exchange with Parahydrogen inside an MRI Scanner. J Phys Chem C. 2017; 121:25994–25999.
10. Barskiy DA, Kovtunov KV, Koptyug IV, He P, Groome KA, Best QA, Shi F, Goodson BM, Shchepin RV, Coffey AM, et al. The Feasibility of Formation and Kinetics of NMR Signal Amplification by Reversible Exchange (SABRE) at High Magnetic Field (9.4 T). J Am Chem Soc. 2014; 136:3322–3325. [PubMed: 24528143]

Author Manuscript Author Manuscript Author Manuscript Author Manuscript

11. Adams RW, Duckett SB, Green RA, Williamson DC, Green GGR. A Theoretical Basis for Spontaneous Polarization Transfer in Non-Hydrogenative Parahydrogen-Induced Polarization. J Chem Phys. 2009; 131:194505. [PubMed: 19929058]
12. Rayner PJ, Burns MJ, Olaru AM, Norcott P, Fekete M, Green GGR, Highton LAR, Mewis RE, Duckett SB. Delivering Strong ^{1}H Nuclear Hyperpolarization Levels and Long Magnetic Lifetimes through Signal Amplification by Reversible Exchange. Proc Natl Acad Sci U S A. 2017:E3188–E3194. [PubMed: 28377523]
13. Atkinson KD, Cowley MJ, Elliott PIP, Duckett SB, Green GGR, Lopez-Serrano J, Whitwood AC. Spontaneous Transfer of Parahydrogen Derived Spin Order to Pyridine at Low Magnetic Field. J Am Chem Soc. 2009; 131:13362–13368. [PubMed: 19719167]
14. Barskiy DA, Shchepin RV, Coffey AM, Theis T, Warren WS, Goodson BM, Chekmenev EY. Over 20% ^{15}N Hyperpolarization in under One Minute for Metronidazole, an Antibiotic and Hypoxia Probe. J Am Chem Soc. 2016; 138:8080–8083. [PubMed: 27321159]
15. Theis T, Ortiz GX, Logan AWJ, Claytor KE, Feng Y, Huhn WP, Blum V, Malcolmson SJ, Chekmenev EY, Wang Q, et al. Direct and Cost-Efficient Hyperpolarization of Long-Lived Nuclear Spin States on Universal $^{15}N_2$-Diazirine Molecular Tags. Sci Adv. 2016; 2:e1501438. [PubMed: 27051867]
16. Colell JFP, Logan AWJ, Zhou Z, Shchepin RV, Barskiy DA, Ortiz GX, Wang Q, Malcolmson SJ, Chekmenev EY, Warren WS, et al. Generalizing, Extending, and Maximizing Nitrogen-15 Hyperpolarization Induced by Parahydrogen in Reversible Exchange. J Phys Chem C. 2017; 121:6626–6634.
17. Theis T, Truong ML, Coffey AM, Shchepin RV, Waddell KW, Shi F, Goodson BM, Warren WS, Chekmenev EY. Microtesla SABRE Enables 10% Nitrogen-15 Nuclear Spin Polarization. J Am Chem Soc. 2015; 137:1404–1407. [PubMed: 25583142]
18. Truong ML, Theis T, Coffey AM, Shchepin RV, Waddell KW, Shi F, Goodson BM, Warren WS, Chekmenev EY. ^{15}N Hyperpolarization by Reversible Exchange Using SABRE-SHEATH. J Phys Chem C. 2015; 119:8786–8797.
19. Shchepin RV, Truong ML, Theis T, Coffey AM, Shi F, Waddell KW, Warren WS, Goodson BM, Chekmenev EY. Hyperpolarization of “Neat” Liquids by NMR Signal Amplification by Reversible Exchange. J Phys Chem Lett. 2015; 6:1961–1967. [PubMed: 26029349]
20. Kovtunov KV, Kovtunova LM, Gemeinhardt ME, Bukhtiyarov AV, Gesiorski J, Bukhtiyarov VI, Chekmenev EY, Koptyug IV, Goodson BM. Heterogeneous Microtesla SABRE Enhancement of ^{15}N NMR Signals. Angew Chem Int Ed. 2017; 56:10433–10437.
21. Colell JFP, Emondts M, Logan AWJ, Shen K, Bae J, Shchepin RV, Ortiz GX, Spannring P, Wang Q, Malcolmson SJ, et al. Direct Hyperpolarization of Nitrogen-15 in Aqueous Media with Parahydrogen in Reversible Exchange. J Am Chem Soc. 2017; 139:7761–7767. [PubMed: 28443329]
22. Logan AWJ, Theis T, Colell JFP, Warren WS, Malcolmson SJ. Hyperpolarization of Nitrogen-15 Schiff Bases by Reversible Exchange Catalysis with Para-Hydrogen. Chem Eur J. 2016; 22:10777–10781. [PubMed: 27218241]
23. Cowley MJ, Adams RW, Atkinson KD, Cockett MCR, Duckett SB, Green GGR, Lohman JAB, Kerssebaum R, Kilgour D, Mewis RE. Iridium N-Heterocyclic Carbene Complexes as Efficient Catalysts for Magnetization Transfer from Para-Hydrogen. J Am Chem Soc. 2011; 133:6134–6137. [PubMed: 21469642]
24. Barskiy DA, Shchepin RV, Tanner CPN, Colell JFP, Goodson BM, Theis T, Warren WS, Chekmenev EY. The Absence of Quadrupolar Nuclei Facilitates Efficient ^{13}C Hyperpolarization Via Reversible Exchange with Parahydrogen. ChemPhysChem. 2017; 18:1493–1498. [PubMed: 28517362]
25. Shchepin RV, Goodson BM, Theis T, Warren WS, Chekmenev EY. Toward Hyperpolarized ^{19}F Molecular Imaging Via Reversible Exchange with Parahydrogen. ChemPhysChem. 2017; 18:1961–1965. [PubMed: 28557156]
26. Vazquez-Serrano LD, Owens BT, Buriak JM. The Search for New Hydrogenation Catalyst Motifs Based on N-Heterocyclic Carbene Ligands. Inorg Chim Acta. 2006; 359:2786–2797.

Author Manuscript Author Manuscript Author Manuscript Author Manuscript

27. Truong ML, Shi F, He P, Yuan B, Plunkett KN, Coffey AM, Shchepin RV, Barskiy DA, Kovtunov KV, Koptyug IV, et al. Irreversible Catalyst Activation Enables Hyperpolarization and Water Solubility for NMR Signal Amplification by Reversible Exchange. J Phys Chem B. 2014; 18:13882–13889.
28. Eshuis N, Aspers RLEG, van Weerdenburg BJA, Feiters MC, Rutjes FPJT, Wijmenga SS, Tessari M. Determination of Long-Range Scalar $^{1}H–^{1}H$ Coupling Constants Responsible for Polarization Transfer in SABRE. J Magn Reson. 2016; 265:59–66. [PubMed: 26859865]
29. Shchepin RV, Barskiy DA, Coffey AM, Feldman MA, Kovtunova LM, Bukhtiyarov VI, Kovtunov KV, Goodson BM, Koptyug IV, Chekmenev EY. Robust Imidazole-$^{15}N_2$ Synthesis for High-Resolution Low-Field (0.05 T) ^{15}N hyperpolarized NMR Spectroscopy. ChemistrySelect. 2017; 2:4478–4483.
30. Barskiy DA, Coffey AM, Nikolaou P, Mikhaylov DM, Goodson BM, Branca RT, Lu GJ, Shapiro MG, Telkki V-V, Zhivonitko VV, et al. NMR Hyperpolarization Techniques of Gases. Chem Eur J. 2017; 23:725–751. [PubMed: 27711999]
31. Pravdivtsev AN, Yurkovskaya AV, Vieth H-M, Ivanov KL, Kaptein R. Level Anti-Crossings Are a Key Factor for Understanding Para-Hydrogen-Induced Hyperpolarization in SABRE Experiments. ChemPhysChem. 2013; 14:3327–3331. [PubMed: 23959909]
32. Ivanov KL, Pravdivtsev AN, Yurkovskaya AV, Vieth H-M, Kaptein R. The Role of Level Anti-Crossings in Nuclear Spin Hyperpolarization. Prog Nucl Mag Res Spectrosc. 2014; 81:1–36.
33. Pravdivtsev AN, Yurkovskaya AV, Lukzen NN, Ivanov KL, Vieth H-M. Highly Efficient Polarization of Spin-1/2 Insensitive NMR Nuclei by Adiabatic Passage through Level Anticrossings. J Phys Chem Lett. 2014; 5:3421–3426. [PubMed: 26278456]
34. Bernatowicz P, Kubica D, Ociepa M, Wodyński A, Gryff-Keller A. Scalar Relaxation of the Second Kind. A Potential Source of Information on the Dynamics of Molecular Movements. 4. Molecules with Collinear C–H and C–Br Bonds. J Phys Chem A. 2014; 118:4063–4070. [PubMed: 24835107]
35. Abragam, A. The Principles of Nuclear Magnetism. Oxford University Press; Oxford, UK: 1961.
36. Kowalewski, J., Maler, L. Nuclear Spin Relaxation in Liquids: Theory, Experiments, and Applications. CRC Press; Boca Raton, FL: 2006. p. 440
37. Blanchard JW, Sjolander TF, King JP, Ledbetter MP, Levine EH, Bajaj VS, Budker D, Pines A. Measurement of Untruncated Nuclear Spin Interactions Via Zero- to Ultralow-Field Nuclear Magnetic Resonance. Phys Rev B. 2015; 92:220202.
38. Erickson SH, Oppenheim GL, Smith GH. Metronidazole in Breast Milk. Obstet Gynecol. 1981; 57:48–50. [PubMed: 7454176]
39. Procissi D, Claus F, Burgman P, Koziorowski J, Chapman JD, Thakur SB, Matei C, Ling CC, Koutcher JA. In Vivo ^{19}F Magnetic Resonance Spectroscopy and Chemical Shift Imaging of Tri-Fluoro-Nitroimidazole as a Potential Hypoxia Reporter in Solid Tumors. Clin Cancer Res. 2007; 13:3738–3747. [PubMed: 17575240]
40. Komar G, Seppänen M, Eskola O, Lindholm P, Grönroos TJ, Forsback S, Sipilä H, Evans SM, Solin O, Minn H. ^{18}F-EF5: A New PET Tracer for Imaging Hypoxia in Head and Neck Cancer. J Nucl Med. 2008; 49:1944–1951. [PubMed: 18997048]
41. Krohn KA, Link JM, Mason RP. Molecular Imaging of Hypoxia. J Nucl Med. 2008; 49
42. Kizaka-Kondoh S, Konse-Nagasawa H. Significance of Nitroimidazole Compounds and Hypoxia-Inducible Factor-1 for Imaging Tumor Hypoxia. Cancer Sci. 2009; 100:1366–1373. [PubMed: 19459851]
43. Fleming IN, Manavaki R, Blower PJ, West C, Williams KJ, Harris AL, Domarkas J, Lord S, Baldry C, Gilbert FJ. Imaging Tumour Hypoxia with Positron Emission Tomography. Br J Cancer. 2015; 112:238–250. [PubMed: 25514380]
44. Masaki Y, Shimizu Y, Yoshioka T, Tanaka Y, Nishijima K-i, Zhao S, Higashino K, Sakamoto S, Numata Y, Yamaguchi Y, et al. The Accumulation Mechanism of the Hypoxia Imaging Probe "FMISO" by Imaging Mass Spectrometry: Possible Involvement of Low-Molecular Metabolites. Sci Rep. 2015; 5:16802. [PubMed: 26582591]

Author Manuscript Author Manuscript Author Manuscript Author Manuscript

45. Zhivonitko VV, Skovpin IV, Koptyug IV. Strong ^{31}P Nuclear Spin Hyperpolarization Produced Via Reversible Chemical Interaction with Parahydrogen. Chem Comm. 2015; 51:2506–2509. [PubMed: 25358646]
46. Olaru AM, Burt A, Rayner PJ, Hart SJ, Whitwood AC, Green GGR, Duckett SB. Using Signal Amplification by Reversible Exchange (SABRE) to Hyperpolarise Sn-119 and Si-29 NMR Nuclei. Chem Comm. 2016; 52:14482–14485. [PubMed: 27904890]
47. Theis T, Truong M, Coffey AM, Chekmenev EY, Warren WS. LIGHT-SABRE Enables Efficient in-Magnet Catalytic Hyperpolarization. J Magn Reson. 2014; 248:23–26. [PubMed: 25299767]
48. Pravdivtsev AN, Yurkovskaya AV, Vieth H-M, Ivanov KL. RF-SABRE: A Way to Continuous Spin Hyperpolarization at High Magnetic Fields. J Phys Chem B. 2015; 119:13619–13629. [PubMed: 25970807]
49. Pravdivtsev AN, Yurkovskaya AV, Zimmermann H, Vieth H-M, Ivanov KL. Transfer of SABRE-Derived Hyperpolarization to Spin-1/2 Heteronuclei. RSC Adv. 2015; 5:63615–63623.
50. Eshuis N, Hermkens N, van Weerdenburg BJA, Feiters MC, Rutjes FPJT, Wijmenga SS, Tessari M. Toward Nanomolar Detection by NMR through SABRE Hyperpolarization. J Am Chem Soc. 2014; 136:2695–2698. [PubMed: 24475903]
51. Eshuis N, Aspers RLEG, van Weerdenburg BJA, Feiters MC, Rutjes FPJT, Wijmenga SS, Tessari M. 2D NMR Trace Analysis by Continuous Hyperpolarization at High Magnetic Field. Angew Chem Int Ed. 2015; 54:14527–14530.
52. Eshuis N, van Weerdenburg BJA, Feiters MC, Rutjes FPJT, Wijmenga SS, Tessari M. Quantitative Trace Analysis of Complex Mixtures Using SABRE Hyperpolarization. Angew Chem Int Ed. 2015; 54:1481–1484.
53. Reile I, Eshuis N, Hermkens N, van Weerdenburg BJA, Feiters MC, Rutjes FPJT, Tessari M. NMR Detection in Biofluid Extracts at Sub-[Small μ]M Concentrations Via Para-H_2 Induced Hyperpolarization. Analyst. 2016; 141:4001–4005. [PubMed: 27221513]
54. Shchepin RV, Barskiy DA, Coffey AM, Goodson BM, Chekmenev EY. NMR Signal Amplification by Reversible Exchange of Sulfur-Heterocyclic Compounds Found in Petroleum. ChemistrySelect. 2016; 1:2552–2555. [PubMed: 27500206]

Author Manuscript Author Manuscript Author Manuscript Author Manuscript

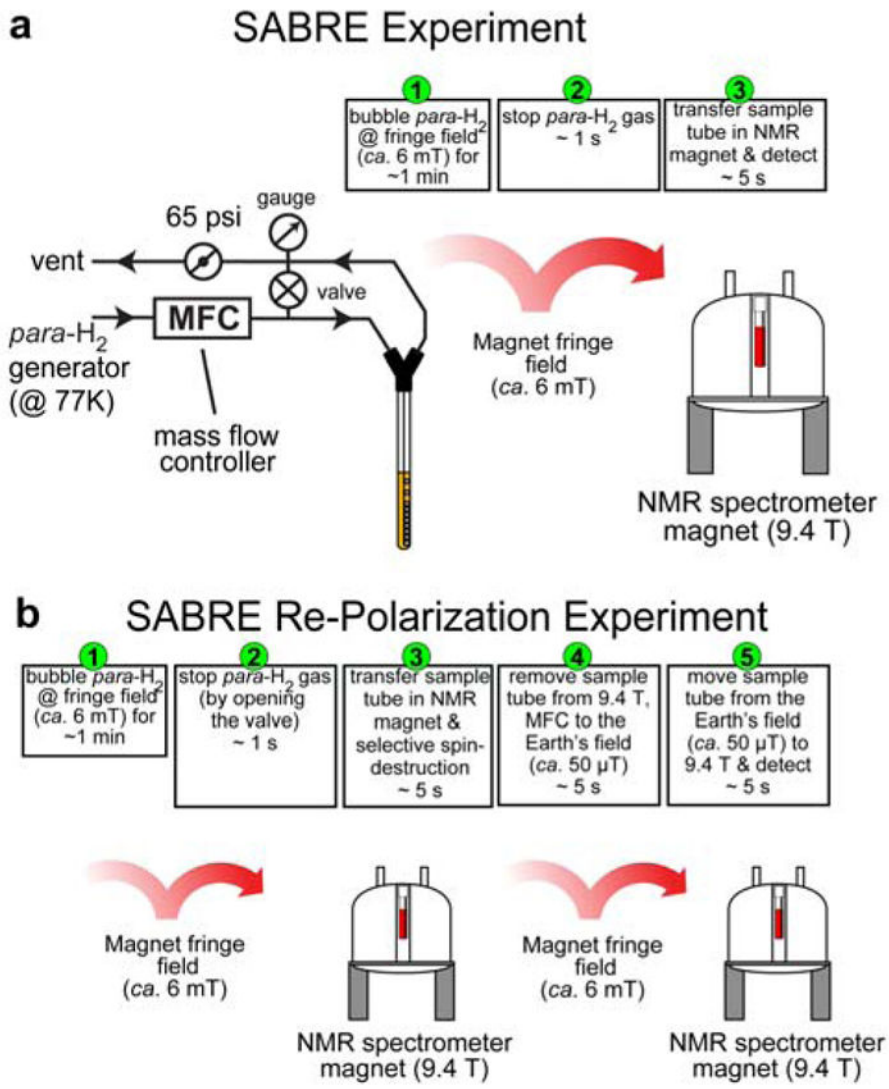

Figure 1.

The schematic of SABRE polarization (a) and re-polarization (b) experiments for ^{1}H hyperpolarization studies.

Author Manuscript
Author Manuscript
Author Manuscript
Author Manuscript

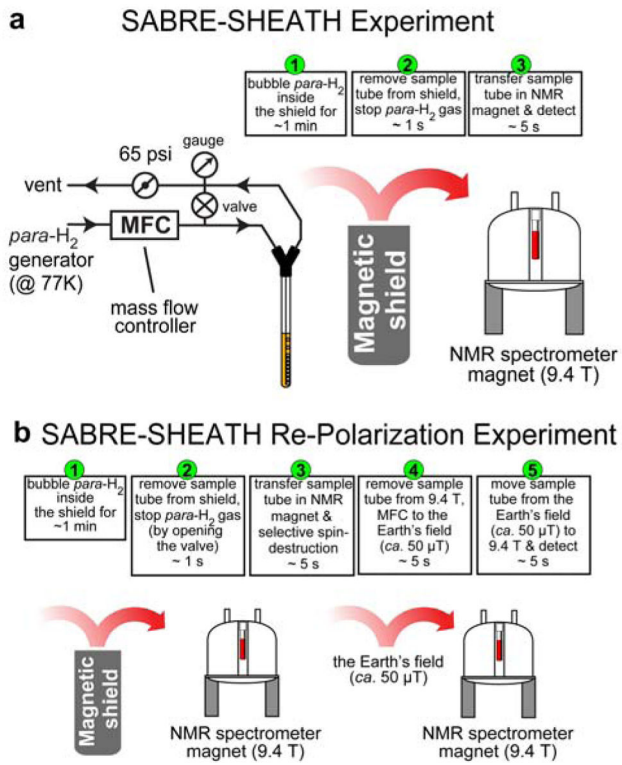

Figure 2.

The schematic of SABRE-SHEATH polarization (a) and re-polarization (b) experiments for ^{15}N and ^{13}C hyperpolarization studies.

Author Manuscript Author Manuscript Author Manuscript Author Manuscript

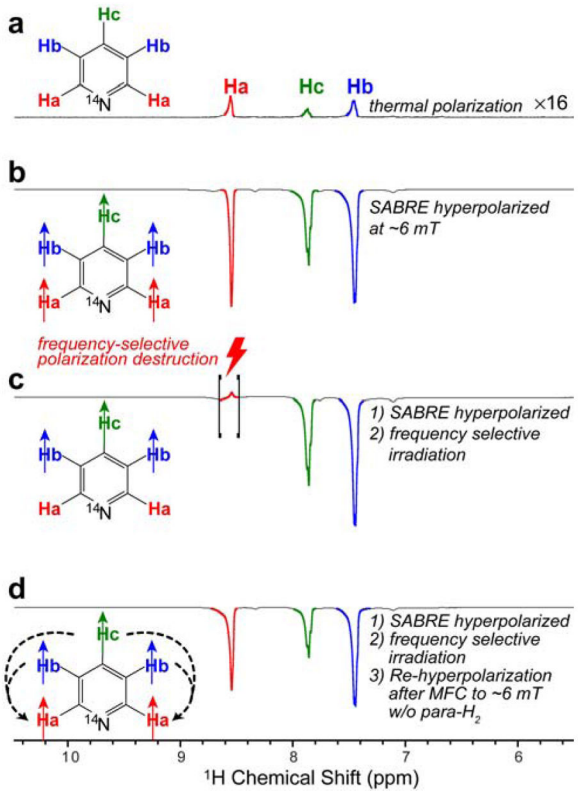

Figure 3.

^{1}H NMR spectra of SABRE-hyperpolarized ~100 mM pyridine solutions in methanol-d_4. All NMR spectra were recorded using Bruker Avance III 9.4 T NMR spectrometer. a) Thermally polarized spectrum provided for signal referencing. b) NMR spectrum of SABRE-hyperpolarized solution (at ~6 mT) after cessation of *para*-H_2 bubbling (Figure 1a). c) NMR spectrum of SABRE-hyperpolarized (at ~6 mT) solution after frequency-selective RF irradiation leading to selective destruction of Ha hyperpolarization; d) the corresponding NMR spectrum after the sample prepared in c) was re-hyperpolarized at ~6 mT without *para*-H_2 bubbling (Figure 1b). We note that the overall signal intensity of the spectrum shown in d) decreased compared to that in spectrum c) due to relaxation processes leading to polarization decay during the additional ~6 s required for sample shuttling. We also note that the total shuttling time (after cessation of *para*-H_2 bubbling) for spectrum d is > 10 s, i.e. more than 3*T_1 of hydrides, and significantly shorter than T_1 of aromatic protons (19±1 s), [10] and therefore, it was concluded that the residual polarization of hydrides cannot serve as a source of re-polarization in spectrum in spectrum d.

Author Manuscript Author Manuscript Author Manuscript Author Manuscript

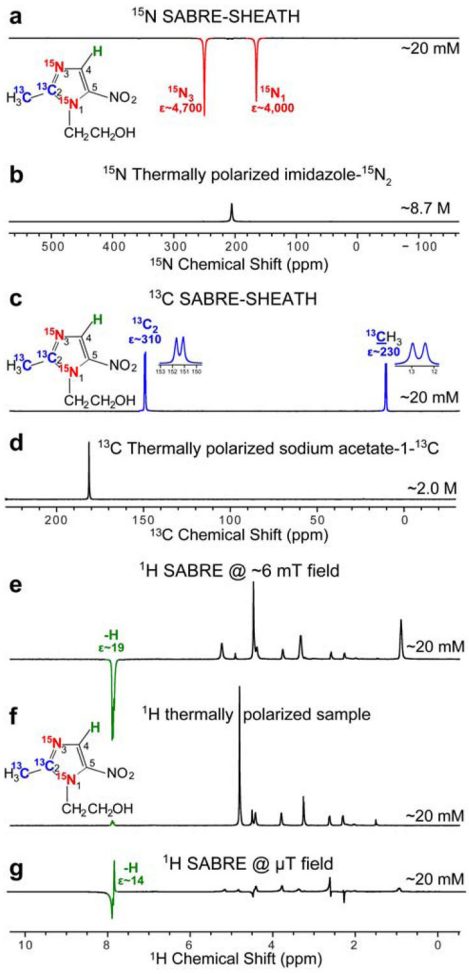

Figure 4.

NMR spectra of metronidazole-$^{15}N_2$-$^{13}C_2$ hyperpolarized using SABRE-SHEATH setup (Figure 2a). a) HP ^{15}N NMR spectrum, b) ^{15}N spectrum from a thermally polarized reference sample, c) HP ^{13}C NMR spectrum, d) ^{13}C spectrum from a thermally polarized reference sample, e) HP ^{1}H NMR spectrum (polarization at ~6 mT), f) ^{1}H spectrum from a thermally-polarized sample, g) HP ^{1}H NMR spectrum (polarization at <1 μT), All spectra were recorded using Bruker Avance III 9.4 T NMR spectrometer.

Author Manuscript Author Manuscript Author Manuscript Author Manuscript

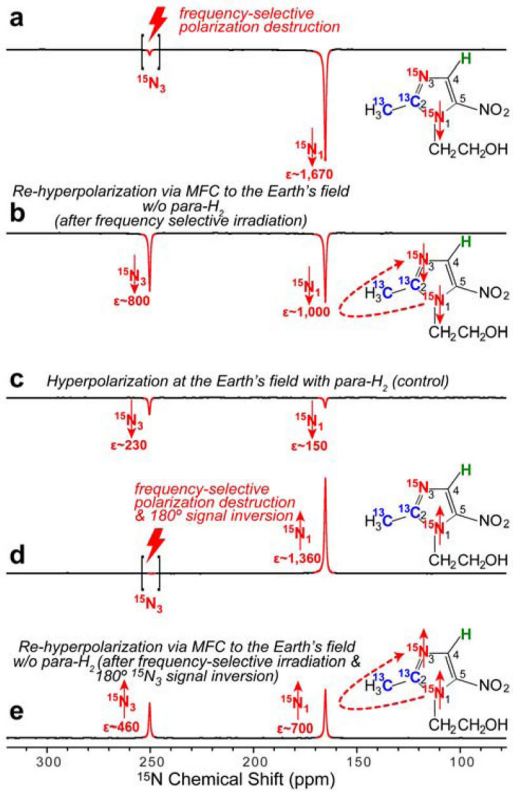

Figure 5.

^{15}N NMR spectra of HP metronidazole-$^{15}N_2$-$^{13}C_2$: a) after SABRE-SHEATH hyperpolarization at μT field, cessation of *para*-H_2 bubbling, and HP sample transfer to the 9.4 T NMR spectrometer followed by frequency-selective polarization destruction of $^{15}N_3$ site. b) the spectrum obtained via the procedure described in (a) followed by magnetic field cycling (MFC) to the Earth's magnetic field and then back to the 9.4 T NMR spectrometer; c) after SABRE hyperpolarization at the Earth's magnetic field, cessation of *para*-H_2 bubbling, and HP sample transfer to the 9.4 T NMR spectrometer; d) the spectrum obtained by the procedure described in (a) followed by 180° phase inversion of the ^{15}N polarization; and e) the spectrum attained by the procedure described in (d), followed by magnetic field cycling (MFC) to the Earth's magnetic field and then returned to the 9.4 T NMR spectrometer. See Figure 2b for details. All NMR spectra are acquired using 90° excitation RF pulse after the respective manipulations.

Author Manuscript Author Manuscript Author Manuscript Author Manuscript

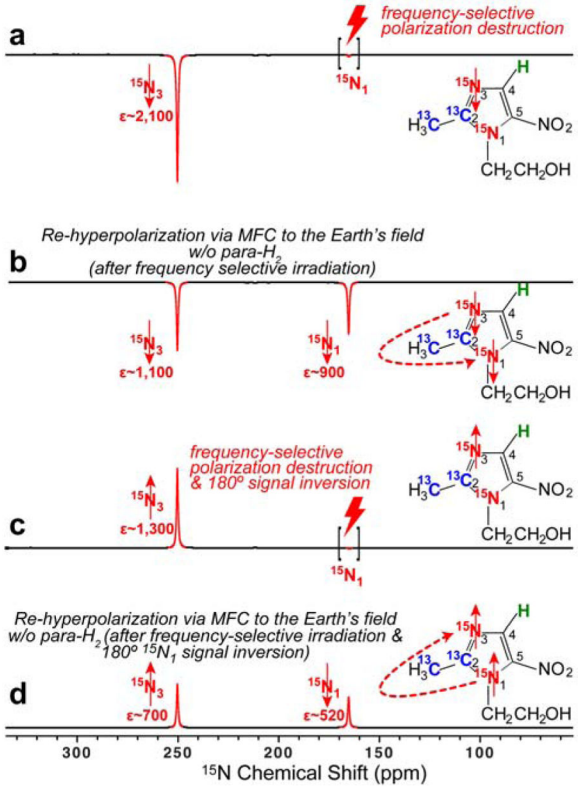

Figure 6.

^{15}N NMR spectra of HP metronidazole-$^{15}N_2$-$^{13}C_2$: a) after SABRE-SHEATH hyperpolarization at μT magnetic field, cessation of *para*-H_2 bubbling, and HP sample transfer into 9.4 T NMR spectrometer followed by frequency-selective polarization destruction of $^{15}N_1$ site; b) the sample produced by the procedure described in (a) followed by the magnetic field cycling (MFC) to the Earth's magnetic field (*ca.* 50 μT) and then back in the 9.4 T NMR spectrometer; c) the sample produced by the procedure described in (a) followed by 180° phase inversion of ^{15}N polarization; d) the sample produced by the procedure described in (c) followed by the magnetic field cycling (MFC) to the Earth's magnetic field (*ca.* 50 μT) and then back in the 9.4 T NMR spectrometer. All NMR spectra are acquired using 90° excitation RF pulse after the respective manipulations.

Author Manuscript Author Manuscript Author Manuscript Author Manuscript

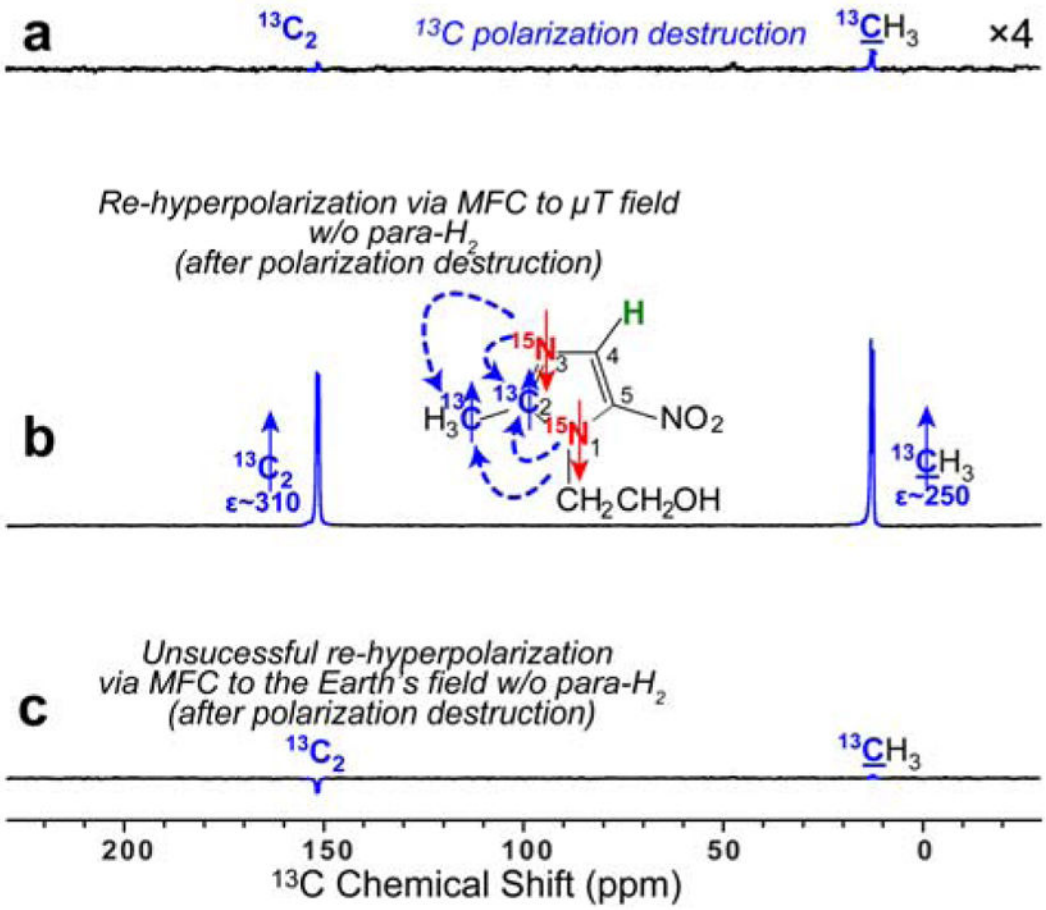

Figure 7.

^{13}C NMR spectra of HP metronidazole-$^{15}N_2$-$^{13}C_2$. a) Spectrum obtained After SABRE-SHEATH hyperpolarization at μT magnetic field, followed by cessation of *para*-H_2 bubbling, and sample transfer to the 9.4 T NMR spectrometer, followed by ^1H and ^{13}C polarization destruction (via applying a series of 90° RF pulses to ^{13}C spins and ^1H decoupling to ^1H spins); b) The spectrum obtained by the procedure described in (a) but followed by magnetic field cycling (MFC) to the μT regime (i.e. within a magnetic shield) and then after the sample was returned to the 9.4 T NMR spectrometer. c) The spectrum obtained by the procedure described in (a) but followed by magnetic field cycling (MFC) to the Earth's magnetic field prior to return to the 9.4 T NMR spectrometer. All NMR spectra shown were acquired using a 90° excitation RF pulse after the respective manipulations described in the figure caption above.

Author Manuscript Author Manuscript Author Manuscript Author Manuscript

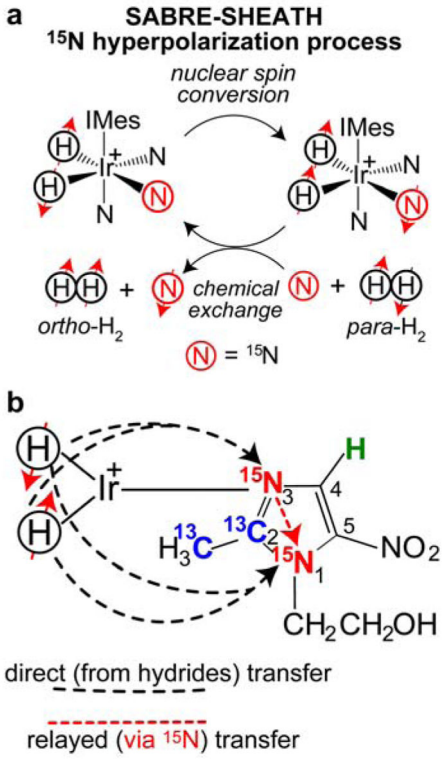

SCHEME 1.

a) The overall schematic of SABRE hyperpolarization of ^{15}N. Spin order is transferred from *para*-H_2 and mediated by scalar spin-spin couplings within a reversibly-formed Ir-IMes hexacoordinate complex.[23, 26] Direct SABRE of short-range ^{15}N sites is accomplished via 2-bond couplings between ^{15}N and hydride protons.[17–18] b) the molecular framework (note axial ligangd of polarization transfer from hydride protons via short- and long-range spin-spin (*J*) couplings.

Author Manuscript Author Manuscript Author Manuscript Author Manuscript

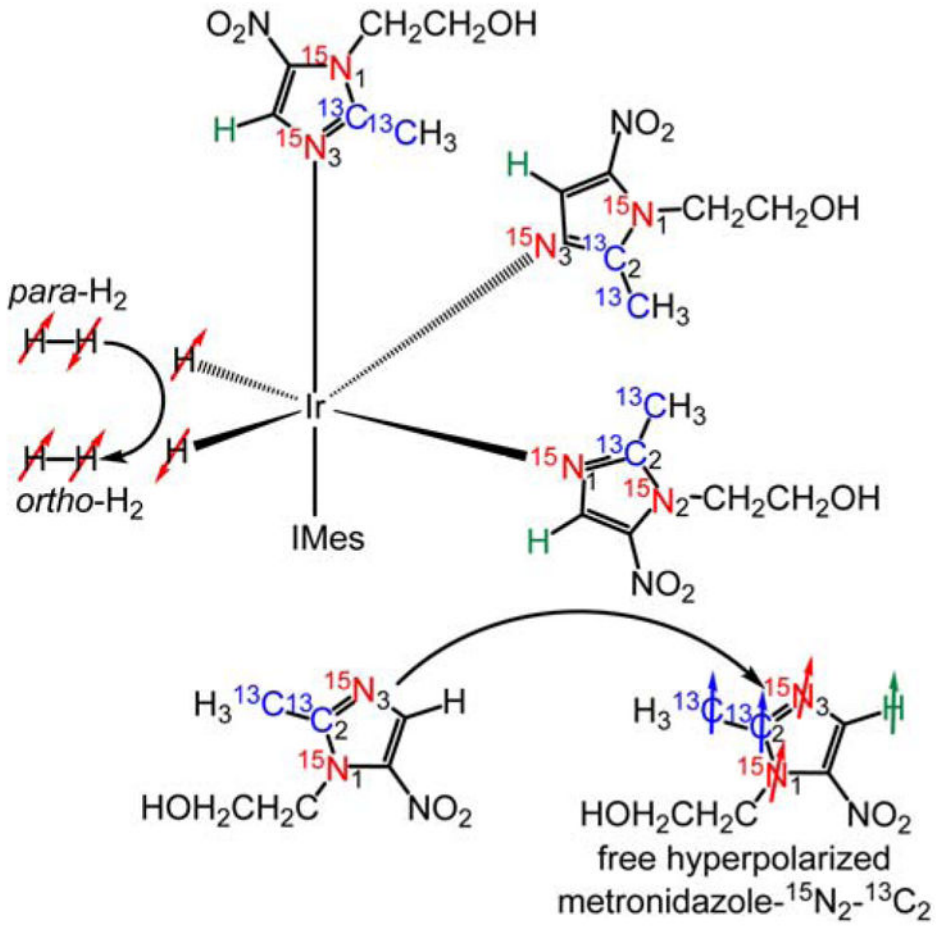

SCHEME 2.

A schematic of the SABRE-SHEATH hyperpolarization process of metronidazole-$^{15}N_2$-$^{13}C_2$ using transfer of spin order from *para*-H_2 on an Ir-IMes hexacoordinate complex.[23, 26] SABRE-SHEATH is accomplished via spin-spin couplings between *para*-H_2-derived hydride protons and nuclear spins of the equatorial exchangeable ligands. The axial ligands are not exchangeable.

Author Manuscript Author Manuscript Author Manuscript Author Manuscript

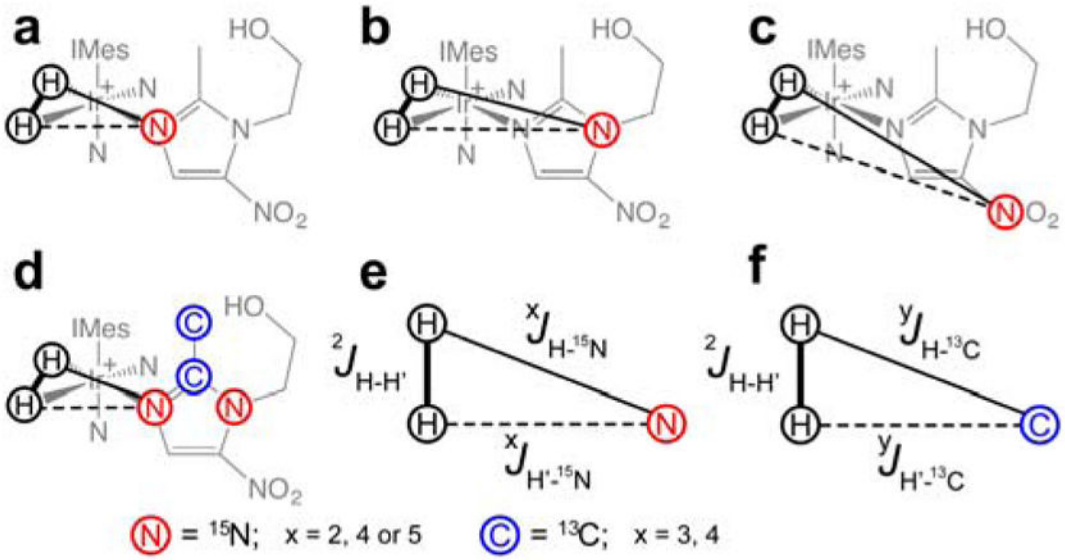

SCHEME 3.

The relevant spin-spin coupling schemes for three ^{15}N sites at natural abundance of ^{15}N and ^{13}C (a–c) and the network for labeled metronidazole-$^{15}N_2$-$^{13}C_2$ (d). Note that only two-bond heteronuclear couplings are shown in d. (e–f) SABRE relevant spin-spin couplings for direct polarization transfer.